

# A model for multiaxial fatigue life prediction based on a new measure of shear stress amplitude

Edgar Nobuo Mamiya, [mamiya@unb.br](mailto:mamiya@unb.br)

Fábio Comes de Castro, [fabiocastro@unb.br](mailto:fabiocastro@unb.br)

Universidade de Brasília, Departamento de Engenharia Mecânica, 70910-900 Brasília, DF, Brazil

**Abstract.** *In this paper, a stress-based model for fatigue life prediction under multiaxial loading conditions is presented. Its main feature is a new measure of shear stress amplitude, defined in terms of the maximum prismatic hull enclosing the stress history — which is capable to take into account the amplitudes in distinct directions of nonproportional multiaxial stress histories. A quadratic combination of the shear stress amplitude with the maximum hydrostatic stress defines an equivalent stress amplitude which is set as an exponential function of the number of cycles to failure (Basquin's rule). An assessment of the model was carried out with experimental data obtained under proportional and nonproportional combinations of normal and shear stresses, with recorded lives ranging from  $7 \times 10^3$  to  $1,13 \times 10^6$  cycles. The results showed good correlations between model predictions and observed lives considering a factor two error band.*

**Keywords:** *Multiaxial fatigue, fatigue life prediction, shear stress amplitude, prismatic hull*

## 1. INTRODUCTION

In real service conditions, the material points of mechanical components are subjected to multiaxial stress histories, which can induce to fatigue failure. Although there are several models reported in the literature, those associated with the concept of critical planes, as for instance the ones proposed by Findley (1959), Fatemi and Socie (1988), McDiarmid (1994) are the most widely used. Their main differences rely upon the equivalent stress or strain amplitude which is considered in the search for the critical plane. More recently, alternative approaches to critical plane models have been proposed. Morel (2000) presented a life prediction model based on the evolution of a mesoscopic damage variable (accumulated plastic strain at grain level). The model proposed by Papadopoulos (2001) considers a generalized shear stress amplitude defined as the volumetric average of the resolved shear stress amplitude over all material planes and gliding directions. Freitas, Li and Santos (2000), as well as Cristofori, Susmel and Tovo (2008) formulated models for life prediction by defining measures of the shear stress amplitudes from the stress path projected into the deviatoric space.

In this paper, we present a new stress-based model for fatigue life prediction under multiaxial loading conditions. Its main feature is a measure of the shear stress amplitude, defined in terms of the maximum prismatic hull enclosing the stress path — which is capable to take into account the amplitudes in distinct directions of nonproportional multiaxial stress paths. A quadratic combination of the shear stress amplitude with the maximum hydrostatic stress defines an equivalent stress amplitude which is set as an exponential function of the number of cycles to failure (Basquin's rule). The model based on the prismatic hull is very efficient in terms of computation time (Mamiya, Araújo and Castro, 2008). This aspect is crucial, for instance, in shape optimization procedures associated with finite element methods, if the objective function includes the life to failure.

The paper is organized as follows: Section 2 introduces the fatigue life estimation model. Section 3 is devoted to the definition of a new shear stress amplitude based on the notion of the largest prismatic hull enclosing the deviatoric part of the stress history. The fatigue model is assessed in Section 4 where experimental observation of fatigue lives for two distinct materials, under in-phase and out-of-phase axial-torsional or bending-torsion loading histories are considered. Finally some concluding remarks are presented in Section 5.

## 2. THE FATIGUE LIFE PREDICTION MODEL

Under uniaxial loading, fatigue life is usually estimated from the Wöhler (or S-N) curve, which associates the stress amplitude with the number of cycles leading to a complete failure of the engineering component. For moderate to long fatigue lives, the S-N curve is often described in terms of the Basquin's rule (Basquin, 1910).

When the material is subjected to multiaxial stress histories, the shear stress amplitude can be associated with a geometrical entity — hyperspheres or ellipsoids, for instance — enclosing the stress history projected into the deviatoric space (Crossland, 1956; Deperrois, 1995; Li, Santos and Freitas, 2000; Zouain, Mamiya and Comes, 2006; Mamiya, Araújo and Castro, 2009). Further, in order to incorporate the effect of tractive normal stress on fatigue life (see Suresh (1998) and references therein), a measure of hydrostatic stress is usually incorporated into the fatigue model. Within this setting, we consider here the following expression for the stress-life rule:

$$S_{eq} := (\tau_a^2 + \kappa \sigma_{Hmax}^2)^{1/2} = \alpha N_f^\beta, \quad (1)$$

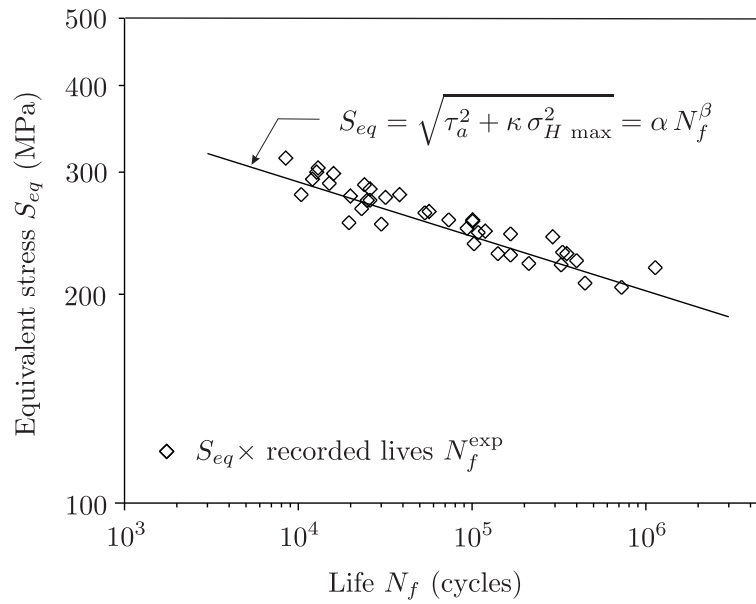


Figure 1. Generalized S-N curve using the prismatic hull as the measure of shear stress amplitude, considering bending and torsion data from Lee (1985).

as illustrated in Fig. 1, where  $S_{eq}$  is an equivalent stress amplitude for multiaxial stress histories, set as a function of the shear stress amplitude  $\tau_a$  — as will be defined in the next section in terms of the prismatic hull enclosing the stress path — and of the maximum hydrostatic stress  $\sigma_{H\ max}$  observed along the loading path. The number of cycles to failure is denoted as  $N_f$ , while  $\kappa$ ,  $\alpha$  and  $\beta$  are material parameters. The quadratic combination of  $\tau_a$  and  $\sigma_{H\ max}$  for the definition of  $S_{eq}$  in (1) was considered so as to obtain a better correlation between estimation and experimental observation of fatigue lives.

### 3. THE PRISMATIC HULL AS A MEASURE OF SHEAR STRESS AMPLITUDE

The life estimation model (1) considers the maximum prismatic hull enclosing the stress path to quantify the shear stress amplitude, as proposed by Mamiya, Araújo and Castro (2008) within the setting of multiaxial fatigue endurance. A detailed presentation of the measure, as well as an algorithm for its calculation, can be found therein. In this section, we describe this measure for the specific case of arbitrary combined normal and shear stresses:

$$\boldsymbol{\sigma}(t) = \begin{bmatrix} \sigma_x(t) & \sigma_{xy}(t) & 0 \\ \sigma_{xy}(t) & 0 & 0 \\ 0 & 0 & 0 \end{bmatrix}. \quad (2)$$

The corresponding history of the deviatoric stress tensor can be written as

$$\mathbf{S}(t) = \frac{1}{3} \begin{bmatrix} 2\sigma_x(t) & 3\sigma_{xy}(t) & 0 \\ 3\sigma_{xy}(t) & -\sigma_x(t) & 0 \\ 0 & 0 & -\sigma_x(t) \end{bmatrix} = s_m(t) \mathbf{m} + s_n(t) \mathbf{n}, \quad (3)$$

where

$$s_m(t) = \frac{2}{\sqrt{6}} \sigma_x(t) \quad \text{and} \quad s_n(t) = \sqrt{2} \sigma_{xy}(t) \quad (4)$$

are the components of the deviatoric stress tensor along directions

$$\mathbf{m} = \frac{1}{\sqrt{6}} \begin{bmatrix} 2 & 0 & 0 \\ 0 & -1 & 0 \\ 0 & 0 & -1 \end{bmatrix} \quad \text{and} \quad \mathbf{n} = \frac{1}{\sqrt{2}} \begin{bmatrix} 0 & 1 & 0 \\ 1 & 0 & 0 \\ 0 & 0 & 0 \end{bmatrix} \quad (5)$$

of an orthonormal basis of the deviatoric space. Figure 2a illustrates a stress path in terms of coordinates  $(s_m(t), s_n(t))$ .

Let us define the *shear stress amplitudes along directions*  $s_{m\theta}$  and  $s_{n\theta}$  as

$$a_{m\theta} = \frac{1}{2} \left( \max_t s_{m\theta}(t) - \min_t s_{m\theta}(t) \right), \quad a_{n\theta} = \frac{1}{2} \left( \max_t s_{n\theta}(t) - \min_t s_{n\theta}(t) \right), \quad (6)$$

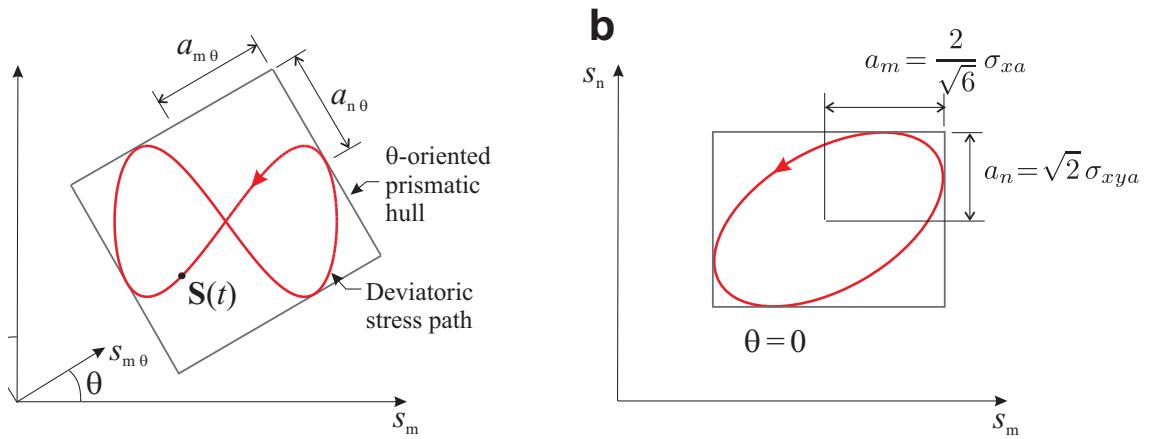


Figure 2. (a) Prismatic hull enclosing an arbitrary stress path in the deviatoric space. (b) Amplitudes  $a_m$  and  $a_n$  in the case of elliptic stress path.

where

$$\begin{bmatrix} s_{m\theta}(t) \\ s_{n\theta}(t) \end{bmatrix} = \begin{bmatrix} \cos \theta & \sin \theta \\ -\sin \theta & \cos \theta \end{bmatrix} \begin{bmatrix} s_m(t) \\ s_n(t) \end{bmatrix}. \quad (7)$$

are the components of the stress path in terms of a coordinate system with orientation  $\theta$ . Notice that the amplitudes defined in (6) are the half sides of the  $\theta$ -oriented prismatic hull enclosing the deviatoric stress path (see Fig. 2a). Next, we set the amplitude of the shear stress path associated with the rotated coordinate system as:

$$\tau_a(\theta) := \frac{1}{\sqrt{2}} \sqrt{a_{m\theta}^2 + a_{n\theta}^2}. \quad (8)$$

Finally, we define the *shear stress amplitude* as the maximum value attained by expression (8) among all orientations  $\theta$ :

$$\tau_a := \max_{0 \leq \theta < 90^\circ} \tau_a(\theta). \quad (9)$$

In the specific case of axial-torsional harmonic loading programs, the components of the stress history (2) can be expressed as

$$\sigma_x(t) = \sigma_{xm} + \sigma_{xa} \sin(\omega t), \quad (10)$$

$$\sigma_{xy}(t) = \sigma_{xym} + \sigma_{xya} \sin(\omega t - \delta), \quad (11)$$

where subscripts  $m$  and  $a$  stand respectively for the mean value and the amplitude of the stress components,  $\omega$  is the loading frequency and  $\delta$  is the phase angle. Since the corresponding deviatoric path is elliptic, the amplitude (8) of the shear stress path is invariant with respect to the orientation  $\theta$  (Mamiya and Araújo, 2002). Thus, if we compute the amplitudes  $a_m$  and  $a_n$  for  $\theta = 0$  (see Fig. 2b),

$$a_m = \frac{2}{\sqrt{6}} \sigma_{xa} \quad \text{and} \quad a_n = \sqrt{2} \sigma_{xya} \quad (12)$$

we obtain

$$\tau_a = \sqrt{\frac{\sigma_{xa}^2}{3} + \sigma_{xya}^2}. \quad (13)$$

Further, the maximum hydrostatic stress in (1) is computed as

$$\sigma_{Hmax} = \frac{1}{3} (\sigma_{xm} + \sigma_{xa}). \quad (14)$$

#### 4. MODEL ASSESSMENT

Multiaxial fatigue tests reported by Lee (1985) and Zhao (2008) are considered for the assessment of the fatigue model proposed in Section 3.

Data from Lee were obtained from bending-torsion deflection-controlled loading programs (10–11) applied upon specimens manufactured from SM45C steel, with reported lives ranging from 8 500 to 1 130 000 cycles. Table 1 describes loading parameters, fatigue lives recorded by Lee along with the ones predicted by our model. Eleven fully reversed bending and ten fully reversed torsion tests were considered for material parameter identification — by a least square fit of the model (1) on life  $N_f$  for each trial parameter  $\kappa$ , together with a minimization of the least square error on  $\kappa$  — producing the following material parameters:

$$\kappa = 1.47, \quad \alpha = 598 \text{ MPa} \quad \text{and} \quad \beta = -0.079. \quad (15)$$

Seventeen in-phase and out-of-phase combined bending and torsion loading programs were considered for the assessment. It can be observed from the graphics in Fig. 3 that prediction and experimental observation of the fatigue lives falls within a factor two error bandwidth for most of the multiaxial data, with a trend towards conservative predictions. Notice also that the correlations between model estimations and experimental observations are confined within the uniaxial (parameter identification) scatter band ( $0.34 \leq N_f^{\text{est}}/N_f^{\text{exp}} \leq 2.82$ ), defined in the same figure by the dashed red lines.

Zhao performed strain controlled axial-torsional tests on 7075-T651 aluminum alloy specimens, with loading histories described by expressions

$$\varepsilon_x(t) = \varepsilon_{xa} \sin(\omega t), \quad (16)$$

$$\gamma_{xy}(t) = \gamma_{xya} \sin(\lambda \omega t - \delta), \quad (17)$$

where  $\lambda$  accounts for the frequency ratio. The reported lives ranged from 7 000 to 920 000 cycles. Table 2 describes strain-driven loading parameters, along with the (stabilized) stress parameters measured at approximately 50% of the failure life. The same table lists the lives recorded by Zhao and Jiang, as well as the ones predicted by our model. It is important to remark, at this point, that our life estimations considered the stress amplitudes in terms of the stabilized stress parameters listed in Table 2. Moreover, as an engineering approach, we assumed that, even within the setting of stabilized elasto-plastic stress-strain relation, the loading path in the deviatoric stress space follows a pattern close to the one imposed in terms of strains. Experimental results which support this assumption can be found, for instance, in the paper communicated by Fatemi and Socie (1988). Five fully reversed traction-compression and nine fully reversed torsional tests were considered for the identification of the following parameters

$$\kappa = 1.95, \quad \alpha = 1237 \text{ MPa} \quad \text{and} \quad \beta = -0.166 \quad (18)$$

of our model. Figure 4 compares predicted versus observed lives for sixteen loading programs, together with the results associated with the tests considered for parameter identification. An inspection of this graphics shows good predictions produced by our model, with all correlations falling within the uniaxial (parameter identification) scatter band ( $0.23 \leq N_f^{\text{est}}/N_f^{\text{exp}} \leq 2.83$ ). Four correlations associated with torsion tests with the presence of mean normal stresses (resulted from plastic shakedown) fall outside the factor two error band. Nevertheless, it should be notice that five of the loading programs considered in the parameter identification process also fall outside the same error band.

## 5. FINAL REMARKS

We proposed, in this paper, a stress-based model for fatigue life prediction under multiaxial loading conditions. Its main feature is a new measure of the shear stress amplitude, defined in terms of the maximum prismatic hull enclosing the stress path, which is capable to take into account the amplitudes in distinct directions of nonproportional multiaxial stress paths. A quadratic combination of the shear stress amplitude with the maximum hydrostatic stress defines an equivalent stress amplitude which is set as an exponential function of the number of cycles to failure (Basquin's rule). Two sets of experimental data for affine as well as multiaxial stress histories were considered for the assessment of the resulting model. The results showed good correlations with observed lives, within a factor two error band as well as the uniaxial (parameter identification) scatter band.

Most of the fatigue models for strain driven loading programs reported in the literature are written in terms of strain parameters, a combination of strain and stress parameters or in terms of dissipated energy (Socie, 2000). On the other hand, there are only a few papers proposing stress-based models which report good correlation with strain driven experimental data (see Lazzarin and Susmel (2003), for instance). As reported in the previous section, our first results show a good correlation with experimental observation for several loading patterns. Nevertheless, we should point out that caution has to be taken when considering stress-based fatigue life models for strain driven loading programs since many open questions still remain. In this context, this paper has to be understood as a preliminary study: in order to obtain a more complete assessment of the model, other materials and loading programs should be considered. The influence of the mean stress upon the fatigue life has also to be addressed. Further, the elasto-plastic behavior of the material under multiaxial loading histories and its consequences upon the fatigue life has to be incorporated into the model.

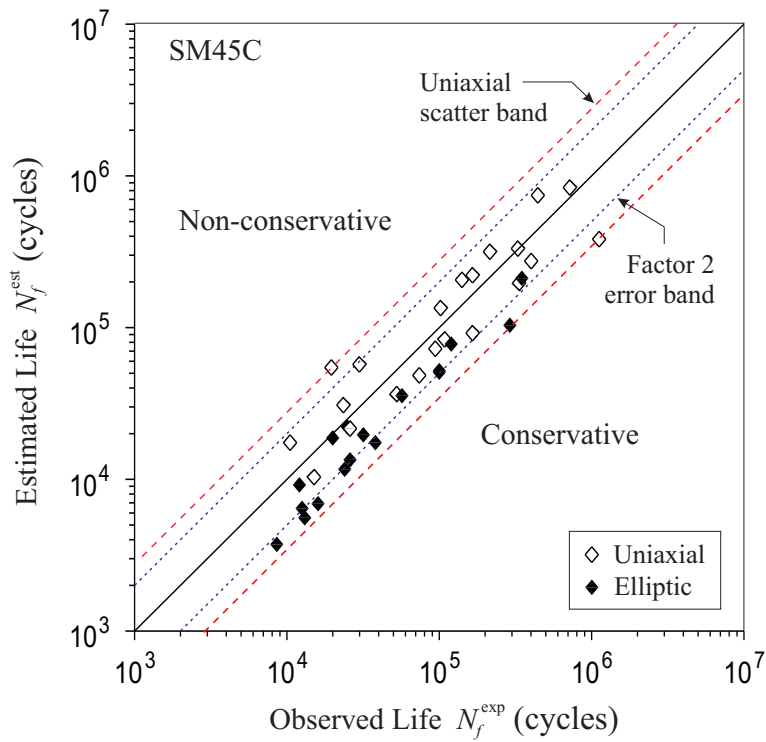


Figure 3. Estimated  $\times$  observed lives for SM45C steel (Lee, 1985).

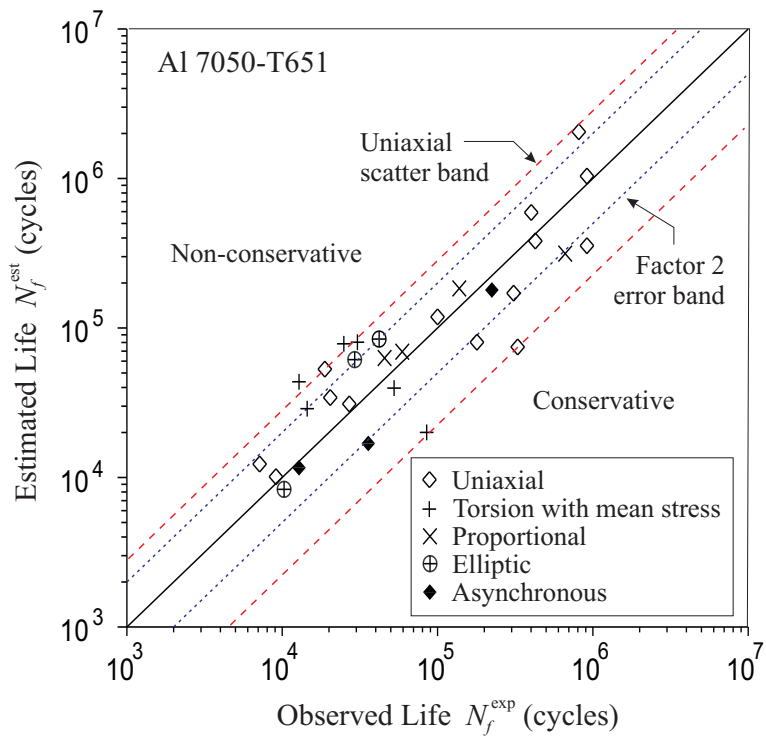


Figure 4. Estimated  $\times$  observed lives for 7075-T651 aluminum alloy (Zhao and Jiang, 2008).

Table 1. Loading parameters and reported lives from fatigue tests performed by Lee (1985) on SM45C steel. Estimated lives  $N_f^{PH}$  from Prismatic Hull model.

| $i$                                     | $\sigma_{xa}$<br>(MPa) | $\sigma_{xm}$<br>(MPa) | $\sigma_{xya}$<br>(MPa) | $\sigma_{xym}$<br>(MPa) | $\delta$<br>( $^\circ$ ) | $N_{fi}^{exp}$<br>(cycles) | $N_{fi}^{PH}$<br>(cycles) |
|---|------------------------|------------------------|-------------------------|-------------------------|--------------------------|----------------------------|---------------------------|
| <i>(a) Fully reversed bending</i>       |                        |                        |                         |                         |                          |                            |                           |
| 1                                       | 411                    | 0                      | 0                       | 0                       | 0                        | 15 000                     | 10 327                    |
| 2                                       | 388                    | 0                      | 0                       | 0                       | 0                        | 26 100                     | 21 508                    |
| 3                                       | 372                    | 0                      | 0                       | 0                       | 0                        | 53 000                     | 36 778                    |
| 4                                       | 364                    | 0                      | 0                       | 0                       | 0                        | 74 000                     | 48 514                    |
| 5                                       | 353                    | 0                      | 0                       | 0                       | 0                        | 93 700                     | 71 719                    |
| 6                                       | 336                    | 0                      | 0                       | 0                       | 0                        | 103 000                    | 134 493                   |
| 7                                       | 323                    | 0                      | 0                       | 0                       | 0                        | 166 000                    | 222 335                   |
| 8                                       | 314                    | 0                      | 0                       | 0                       | 0                        | 213 000                    | 318 678                   |
| 9                                       | 313                    | 0                      | 0                       | 0                       | 0                        | 327 000                    | 331 894                   |
| 10                                      | 294                    | 0                      | 0                       | 0                       | 0                        | 445 000                    | 736 992                   |
| 11                                      | 291                    | 0                      | 0                       | 0                       | 0                        | 723 000                    | 839 859                   |
| <i>(b) Fully reversed torsion</i>       |                        |                        |                         |                         |                          |                            |                           |
| 12                                      | 0                      | 0                      | 278                     | 0                       | 0                        | 10 400                     | 17 423                    |
| 13                                      | 0                      | 0                      | 266                     | 0                       | 0                        | 23 300                     | 30 567                    |
| 14                                      | 0                      | 0                      | 254                     | 0                       | 0                        | 19 500                     | 55 036                    |
| 15                                      | 0                      | 0                      | 253                     | 0                       | 0                        | 30 000                     | 57 872                    |
| 16                                      | 0                      | 0                      | 246                     | 0                       | 0                        | 109 000                    | 82 737                    |
| 17                                      | 0                      | 0                      | 244                     | 0                       | 0                        | 166 000                    | 91 804                    |
| 18                                      | 0                      | 0                      | 230                     | 0                       | 0                        | 332 000                    | 194 883                   |
| 19                                      | 0                      | 0                      | 229                     | 0                       | 0                        | 142 000                    | 206 006                   |
| 20                                      | 0                      | 0                      | 224                     | 0                       | 0                        | 403 000                    | 272 907                   |
| 21                                      | 0                      | 0                      | 218                     | 0                       | 0                        | 1 130 000                  | 385 680                   |
| <i>(c) Combined bending and torsion</i> |                        |                        |                         |                         |                          |                            |                           |
| 22                                      | 390                    | 0                      | 151                     | 0                       | 0                        | 8 500                      | 2 754                     |
| 23                                      | 349                    | 0                      | 148                     | 0                       | 0                        | 24 000                     | 11 584                    |
| 24                                      | 325                    | 0                      | 153                     | 0                       | 0                        | 32 000                     | 19 599                    |
| 25                                      | 372                    | 0                      | 93                      | 0                       | 0                        | 38 000                     | 17 286                    |
| 26                                      | 309                    | 0                      | 134                     | 0                       | 0                        | 100 000                    | 50 573                    |
| 27                                      | 265                    | 0                      | 225                     | 0                       | 90                       | 12 000                     | 9 152                     |
| 28                                      | 392                    | 0                      | 118                     | 0                       | 90                       | 12 700                     | 6 490                     |
| 29                                      | 417                    | 0                      | 78                      | 0                       | 90                       | 13 000                     | 5 565                     |
| 30                                      | 346                    | 0                      | 173                     | 0                       | 90                       | 16 000                     | 6 896                     |
| 31                                      | 245                    | 0                      | 216                     | 0                       | 90                       | 20 000                     | 18 641                    |
| 32                                      | 245                    | 0                      | 211                     | 0                       | 90                       | 25 000                     | 22 326                    |
| 33                                      | 304                    | 0                      | 186                     | 0                       | 90                       | 26 000                     | 13 442                    |
| 34                                      | 304                    | 0                      | 152                     | 0                       | 90                       | 57 000                     | 35 860                    |
| 35                                      | 314                    | 0                      | 127                     | 0                       | 90                       | 100 000                    | 51 974                    |
| 36                                      | 286                    | 0                      | 143                     | 0                       | 90                       | 120 000                    | 78 036                    |
| 37                                      | 167                    | 0                      | 211                     | 0                       | 90                       | 290 000                    | 104 102                   |
| 38                                      | 265                    | 0                      | 132                     | 0                       | 90                       | 350 000                    | 209 508                   |

## 6. ACKNOWLEDGEMENTS

The support provided by CNPq under contract 308916/2006-9 is gratefully acknowledged.

## 7. REFERENCES

- Basquin, O.H., 1910, "The exponential law of endurance test", Proc. Annual Meeting, American Society for Testing Materials, Vol. 10, pp. 625-630.
- Cristofori, A., Susmel, L. and Tovo, R., 2008, "A stress invariant based criterion to estimate fatigue damage under multi-axial loading", International Journal of Fatigue, Vol. 30, pp. 1646-1658.
- Crossland, B., 1956, "Effect of Large Hydrostatic Pressures on The Torsional Fatigue Strength of an Alloy Steel", Proc. Int. Conf. on Fatigue of Metals, Institution of Mechanical Engineers, London, pp. 138-149.
- Deperrois, A., 1995, "Sur le Calcul de Limites d'Endurance des Aciers", Ecole Polytechnique, Ph.D. Thesis.

Table 2. Loading parameters and reported lives from fatigue tests performed by Zhao and Jiang (2008) on 7075-T651 aluminum alloy. Estimated lives  $N_f^{PH}$  from Prismatic Hull model.

| $i$  | $\varepsilon_{xa}$ | $\gamma_{xya}$ | $\delta$<br>(°) | $\lambda$ | $\sigma_{xa}$<br>(MPa) | $\sigma_{xm}$<br>(MPa) | $\sigma_{xya}$<br>(MPa) | $N_{fi}^{exp}$<br>(cycles) | $N_{fi}^{PH}$<br>(cycles) |
|--|--------------------|----------------|-----------------|-----------|------------------------|------------------------|-------------------------|----------------------------|---------------------------|
| <i>(a) Fully reversed traction-compression</i> |                    |                |                 |           |                        |                        |                         |                            |                           |
| 1  | 0.49               | 0              | 0               | 1         | 349.7                  | 0.0                    | 0                       | 7 144                      | 12 286                    |
| 2  | 0.51               | 0              | 0               | 1         | 361.6                  | -3.6                   | 0                       | 9 112                      | 10 043                    |
| 3  | 0.42               | 0              | 0               | 1         | 299.6                  | 1.5                    | 0                       | 27 011                     | 31 209                    |
| 4  | 0.34               | 0              | 0               | 1         | 240.0                  | 1.1                    | 0                       | 99 287                     | 118 848                   |
| 5  | 0.28               | 0              | 0               | 1         | 200.2                  | 0.6                    | 0                       | 919 687                    | 354 565                   |
| <i>(b) Fully reversed torsion</i>              |                    |                |                 |           |                        |                        |                         |                            |                           |
| 6  | 0                  | 0.75           | 0               | 1         | 0                      | 0                      | 203.3                   | 18 842                     | 53 320                    |
| 7  | 0                  | 0.80           | 0               | 1         | 0                      | 0                      | 219.0                   | 20 271                     | 34 052                    |
| 8  | 0                  | 0.69           | 0               | 1         | 0                      | 0                      | 190.3                   | 178 065                    | 79 413                    |
| 9  | 0                  | 0.60           | 0               | 1         | 0                      | 0                      | 167.8                   | 308 144                    | 169 557                   |
| 10   | 0                  | 0.69           | 0               | 1         | 0                      | 0                      | 192.0                   | 328 816                    | 75 268                    |
| 11   | 0                  | 0.50           | 0               | 1         | 0                      | 0                      | 136.5                   | 403 731                    | 588 575                   |
| 12   | 0                  | 0.55           | 0               | 1         | 0                      | 0                      | 146.9                   | 428 510                    | 378 066                   |
| 13   | 0                  | 0.40           | 0               | 1         | 0                      | 0                      | 110.8                   | 805 783                    | 2 069 733                 |
| 14   | 0                  | 0.46           | 0               | 1         | 0                      | 0                      | 124.5                   | 913 545                    | 1 024 965                 |
| <i>(c) Torsion, with mean stress</i>           |                    |                |                 |           |                        |                        |                         |                            |                           |
| 15   | 0.69               | 0              | 0               | 1         | 0                      | 200.                   | 188.5                   | 12 739                     | 43 558                    |
| 16   | 0.69               | 0              | 0               | 1         | 0                      | -200.                  | 192.0                   | 52 986                     | 39 830                    |
| 17   | 0.69               | 0              | 0               | 1         | 0                      | -293.1                 | 196.7                   | 84 946                     | 19 914                    |
| 18   | 0.50               | 0              | 0               | 1         | 0                      | 289.8                  | 134.2                   | 30 192                     | 79 466                    |
| 19   | 0.50               | 0              | 0               | 1         | 0                      | 288.7                  | 135.4                   | 25 167                     | 78 250                    |
| 20   | 0.50               | 0              | 0               | 1         | 0                      | 391.6                  | 131.6                   | 14 489                     | 29 071                    |
| <i>(d) Proportional</i>                        |                    |                |                 |           |                        |                        |                         |                            |                           |
| 21   | 0.17               | 0.60           | 0               | 1         | 127.2                  | 0                      | 170.5                   | 59 194                     | 68 856                    |
| 22   | 0.23               | 0.40           | 0               | 1         | 166.1                  | 0                      | 110.4                   | 136 646                    | 184 837                   |
| 23   | 0.28               | 0.49           | 0               | 1         | 201.3                  | 0                      | 130.0                   | 45 500                     | 62 606                    |
| 24   | 0.21               | 0.37           | 0               | 1         | 153.5                  | 0                      | 100.3                   | 662 627                    | 311 190                   |
| <i>(e) 90 degrees out-of-phase</i>             |                    |                |                 |           |                        |                        |                         |                            |                           |
| 25   | 0.38               | 0.66           | 90              | 1         | 280.4                  | 0                      | 181.8                   | 10 191                     | 8 403                     |
| 26   | 0.28               | 0.49           | 90              | 1         | 200.9                  | 0                      | 131.6                   | 29 439                     | 61 043                    |
| 27   | 0.27               | 0.41           | 90              | 1         | 200.6                  | 0                      | 115.8                   | 41 747                     | 84 028                    |
| <i>(f) Asynchronous</i>                        |                    |                |                 |           |                        |                        |                         |                            |                           |
| 28   | 0.28               | 0.49           | 0               | 2         | 205.8                  | 0                      | 137.5                   | 35 804                     | 16 712                    |
| 28   | 0.20               | 0.32           | 0               | 2         | 147.5                  | 0                      | 86.9                    | 225 000                    | 178 522                   |
| 30   | 0.28               | 0.49           | 0               | 4         | 203.8                  | 0                      | 136.3                   | 12 708                     | 11 267                    |

Fatemi, A., Socie, D.F., 1988, "A critical plane approach to multiaxial fatigue damage including out-of-phase loading", *Fatigue and Fracture of Engineering Materials and Structures*, Vol. 11, No. 3, pp. 149-165.

Findley, W.N., 1959, "A theory for the effect of mean stress on fatigue of metals under combined torsion and axial load and bending", *Journal of Engineering for Industry*, pp. 301-306.

Freitas, M., Li, B. and Santos, J.L.T., 2000, "A numerical approach for high-cycle fatigue life prediction with multiaxial loading, in: S. Kalluri and P. J. Bonacuse, editors, *Multiaxial Fatigue and Deformation: Testing and Prediction*, ASTM STP 1387, pp. 139-156.

Lazzarin, P. and Susmel, L., 2003, "A stress-based method to predict lifetime under multiaxial fatigue loadings", *Fatigue and Fracture of Engineering Materials and Structures*, Vol. 26, pp. 1171-1187.

Lee, S.-B., 1985, "A Criterion for Fully Reversed Out-of-Phase Torsion and Bending", *Multiaxial Fatigue*, ASTM STP 853, K. J. Miller and M. W. Brown, Eds., American Society for Testing and Materials, Philadelphia, pp. 553-568.

Li, B., Santos, J.L.T. and Freitas, M., 2000, "A unified numerical approach for multiaxial fatigue limit evaluation", *Int. J. of Mechanics of Structures and Machines*, Vol. 28, pp. 85-103.

Mamiya, E.N., Araújo, J.A. and Castro, F.C., 2009, "Prismatic hull: A new measure of shear stress amplitude in multiaxial high cycle fatigue", *International Journal of Fatigue*, Vol.31, pp. 1144-1153.

McDiarmid, D.L., 1994, "A shear-stress based critical-plane criterion of multiaxial fatigue failure for design and life prediction", *Fatigue and Fracture of Engineering Materials and Structures*, Vol. 17, pp. 1475-1484.

- Morel, F., 2000, "A critical plane fatigue model applied to out-of-phase bending and torsion load conditions", *Fatigue and Fracture of Engineering Materials and Structures*, Vol. 24, pp. 153-164.
- Papadopoulos I.V., 2001, "Long life fatigue under multiaxial loading", *International Journal of Fatigue*, Vol. 23, pp. 839-849.
- Socie, D.F. and Marquis, G.B., 2000, "Multiaxial fatigue", SAE International.
- Suresh, S., 1998, "Fatigue of Materials", Cambridge University Press, 2nd Edition.
- Zhao, T. and Jiang, Y., 2008, "Fatigue of 7075-T651 Aluminum Alloy", *International Journal of Fatigue*, Vol.30, pp. 834-849.
- Zouain, N., Mamiya, E.N. and Comes, F., 2006, "Using enclosing ellipsoids in multiaxial fatigue strength criteria", *European Journal of Mechanics - A/Solids*, Vol. 25, pp. 51-71.

## **8. Responsibility notice**

The authors are the only responsible for the printed material included in this paper.